JOURNAL OF AIRCRAFT
Vol. 47, No. 1, January–February 2010

Engineering Notes

Bat-Inspired Wing Aerodynamics and Optimization

Emily A. Leylek,* Justin E. Manzo,† and Ephrahim Garcia‡
Cornell University, Ithaca, New York, 14853

DOI: 10.2514/1.41374

I. Introduction

AS ENGINEERS search to make micro air vehicles more stable, maneuverable, and efficient, many are turning toward biology for inspiration. Bats adapt to their environment by morphing their wings in flight. Depending on their niche, certain species soar and glide [1], whereas others perform barrel rolls in nature [2] and can pull up to 4.5 g in obstacle courses [3]. Morphological changes afford bats great agility at low speeds, and they are able to maintain stability and control at low Reynolds numbers, in which viscous effects and leading edge laminar separation bubbles cause nonlinearities in lift [4–6]. Bats achieve these feats with fingerlike jointed bone structures and flexible wing membranes. These unique traits allow them to change camber and twist in flight, unlike avian span changes.

Recent studies investigate replicating flapping bat flight [7–9], whereas others focus specifically on flexible, membrane wing benefits at low Reynolds numbers for improvements in gust alleviation and delayed stall characteristics [10–12]. These wings are passive elements, and it is difficult to attach control surfaces to them for flight authority. By actively controlling and morphing flexible wings, conventional controllers can be replaced. Aircraft morphing allows single vehicles to have multiple functions, ideally with continuous lifting surfaces to alleviate drag and vibration and increase efficiency. This is the focus of Garcia et al. [13], which proposes a nonflapping wing with twist capabilities. Morphing enables tailoring of wing shapes to multiple flight regimes, from takeoff through cruise to landing [14–16]. Many mechanisms have been proposed for morphing, such as the smart joint, an active rigidity composite suited to actuating a batlike membrane wing in flight [17]. This low-profile device can be embedded at joints in the fingerlike skeletal wing structure as a bimorph actuator [18]. Whereas this work focuses on static wing configurations rather than morphing behavior, results help specify actuator requirements used for a variable camber and twist wing.

In this work, two key features of bat flight are studied, uniquely evolved bat wing planforms adapted to environments, and capabilities afforded through variable camber and twist, and are applied to rigid, fixed wing designs for small man-made craft. The goal of this study is not to mimic natural bat flight, but to understand how certain aspects of bat flight apply to the engineering problem of wing design for micro air vehicles.

Received 2 Oct. 2008; revision received 2 Sept. 2009; accepted for publication 13 Sept. 2009.

*Undergraduate Student, Sibley School of Mechanical and Aerospace Engineering, 226 Upson Hall.

†Graduate Student, Sibley School of Mechanical and Aerospace Engineering, 226 Upson Hall.

‡Associate Professor, Sibley School of Mechanical and Aerospace Engineering, 224 Upson Hall. Member AIAA.

II. Background and Motivation

To perform maneuvers unprecedented in animal flight, bats primarily control wing shape by using the fifth digit of their handlike bone structure to vary camber, analogous to conventional aircraft flaps [1–3,19–22]. They also create leading edge slats using their thumb and propatagium, the wing membrane in front of the arm. This device also changes wing camber, helps keep the boundary layer attached, and prevents flow separation, particularly at high angle-of-attack α [3,21,22]. To initiate turns, bats morph their wings to create asymmetric lift, increasing α on one wing and decreasing it on the other by modifying twist distribution. Asymmetric lift distribution is also achieved by increasing or negating camber, or by stalling all or part of one wing. These twist and camber morphology changes and their aerodynamic effects on bat wing planforms are the focus of this research.

A. Morphological Correlations to Flight Performance

Maneuverability is defined as the space required for turns at fixed speed, and agility is maximum roll acceleration available to initiate a turn [2]. Wings favoring maneuverability have large area, low aspect ratio, and rounded wingtips. Similar to human aircraft, agile wings produce large rolling torque by creating asymmetric lift as described earlier. This is accomplished either by reducing wing inertia or by creating large rolling moments [2]. Bat flight performance can also be measured by cost of transport, a measure of efficiency. Highly efficient bat wings require minimal thrust and produce minimal drag, factors particularly important for migratory or commuting bats. Their wings usually have a high aspect ratio and pointed wingtips [2]. Generally, bat wings are not this simply defined and represent additional morphological adaptations to succeed in their niche.

B. Bat Species Studied

In this research, three diverse species are selected, embodying different wing forms and flight functions. Performance of these species is compared, including evaluation of wing morphing utility. Wing planforms are shown in Fig. 1, extracted from Norberg et al. [1] and Norberg and Rayner [2].

The first bat of Fig. 1 is the piscivorous (fish-hunting) *Noctilio leporinus*. Its high aspect ratio wing allows efficient flight during commutes to water sources but also has large, rounded wingtips providing stability and control for prey capture [2]. *Pteropus livingstonii* is a soaring fruit bat, with midrange aspect ratio and pointed wingtips for increased efficiency [1]. *Nycteris hispida* hunts for insects in heavy vegetation, with short wings of low aspect ratio. Its flight is slow but maneuverable and agile, with large, rounded wingtips [2]. The shape of the wings suggests that *Noctilio leporinus* combines characteristics for low cost of transport with maneuverability, *Pteropus livingstonii* is evolved for efficient flight, and *Nycteris hispida* has wings designed for high maneuverability and agility.

III. Computational Analysis

Wing topology, in the form of quarter chord location and chord length distribution, was measured from reference drawings [1,2] using CorelDraw 8.0 and entered into MATLAB to create digital planforms (Fig. 1). Diverging from natural flapping flight to fixed wing designs, topology is mapped onto a solid airfoil distribution. An in-house lifting-line analysis is used to evaluate the flight characteristics of entire wings [23].

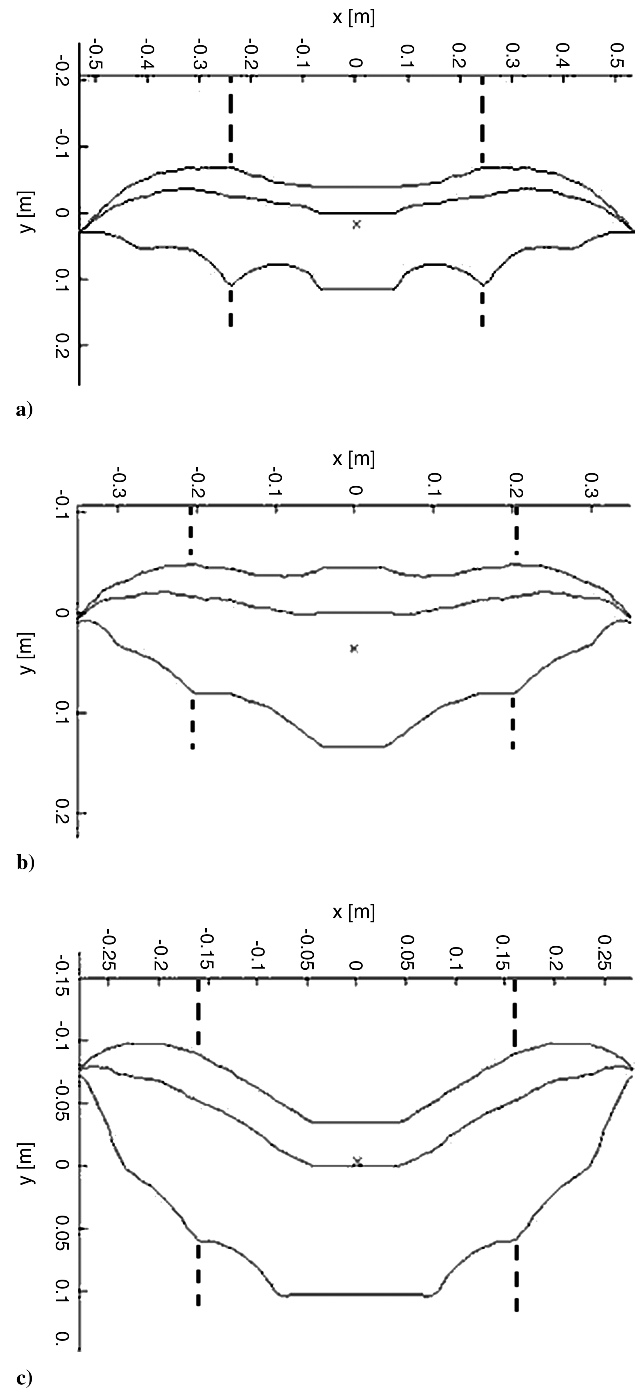

Fig. 1 Bat wing planforms studied, fifth finger location at dashed lines: a) *Noctilio leporinus*, b) *Pteropus livingstonii*, c) *Nycteris hispida*.

A. Methodology

Data based on XFOIL studies best determine airfoil distribution using thin, cambered NACA airfoils. XFOIL is a computational solver for 2-D airfoils combining an inviscid panel method with a boundary layer formulation to predict lift, drag, and pitching moment for airfoils in viscous flows [24]. Airfoils of the 4-digit NACA family, all with 3% thickness-to-chord ratio and maximum camber located at 30% chord (NACA $x303$), are investigated to study how camber affects lift coefficient and lift-to-drag ratio for low Reynolds numbers. The turbulence transition is free, and wings are studied at a Reynolds number of 10^5, the upper end of bat and micro air vehicle (MAV) flight regimes ($10^4 - 10^5$) [11,20]. Results of this study are presented in Leylek et al. [25]. In addition to thickness limitations prohibiting quasi-membrane study, XFOIL is known to overpredict lift and underpredict drag, a common result yielding artificially enhanced theoretical results [4].

A lifting-line analysis, based on Weissinger's method for straight, swept wings, decomposes 3-D wings into a series of 2-D airfoils. Each bat wing consists of 101 spanwise stations, with lifting line assumed at the quarter chord point. Potential flow theory calculates wing circulation and consequent lift by relating downwash at each station to horseshoe vortex intensity acting at the quarter chord and projected to a semi-infinite trailing vortex sheet [23]. This method allows for curved wing planforms, taking into account variable profile wing shapes by incorporating look-up tables for 2-D airfoil data from XFOIL. The code yields lift and drag forces, as well as pitch, roll, and yaw moments. Lifting-line analysis assumes a planar trailing vortex sheet and, being a potential flow method, is valid at high Reynolds numbers with minimal viscous effects and no separation [23]. However, using airfoil data incorporating XFOIL's boundary layer formulation account for some viscous effects apparent in low Reynolds number flight. Although numerical solutions may not be exact, the code has utility for initial design and comparison of wing shapes given its speed and simplicity.

Each wing is scaled by mean chord to a Reynolds number of 10^5 flying at 10 m/s, matching bat flight speeds. Two topologies are tested for each species' planform, an unmorphed and a morphed snapshot. The unmorphed shape is a flat wing, consisting of symmetric NACA 0003 airfoils without twist to be a baseline for comparison. The morphed configuration models bat wing shapes in gliding flight, graphically interpolated from flight images as an initial guess for morphed wing shape used in analysis. Camber and twist distributions provide sufficient information to prescribe 3-D wing shapes from digitized planforms.

For the morphed wing shape, the midsection representing bat body is assumed to produce zero lift in level flight, such that root is an untwisted NACA 0003 airfoil. A NACA 7303 airfoil is placed at the fifth digit, representing camber actuation marked by dashed locations in Fig. 1. This airfoil is selected through XFOIL study as having the highest lift-to-drag ratio, a requirement for gliding. Wingtip profile assumes airfoils of 1% camber, or NACA 1303. Airfoil distribution is indicated by points A, B, and C in Fig. 2 for each wing, with linear interpolation between points. Regions of positive and negative twist are shown qualitatively in Fig. 2, magnified for clarity. Observed in bat flight images, at the fifth digit the wing trailing edge deflects

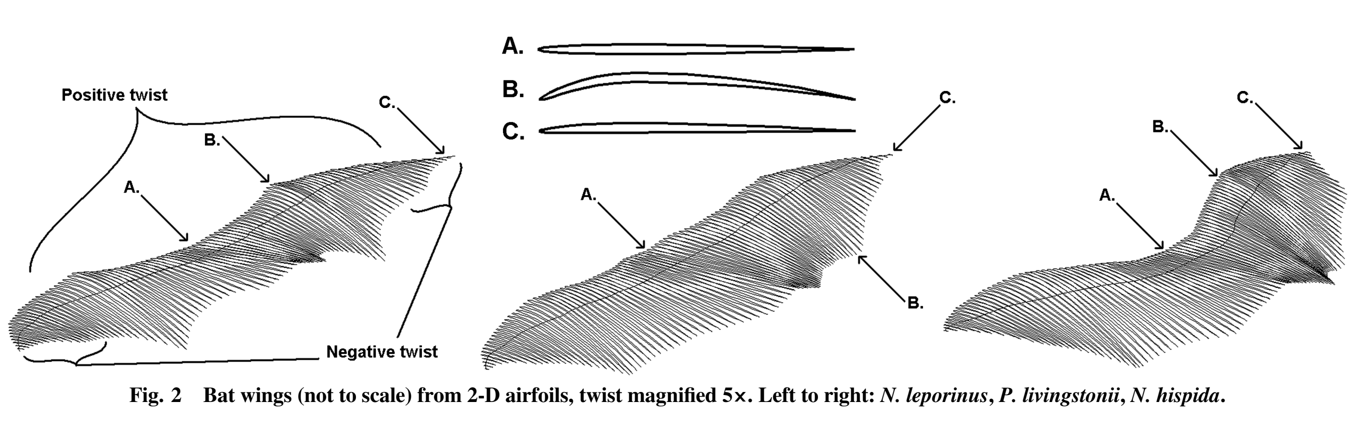

Fig. 2 Bat wings (not to scale) from 2-D airfoils, twist magnified 5×. Left to right: *N. leporinus*, *P. livingstonii*, *N. hispida*.

below the X-Y plane and the leading edge deflects upward, while at the tips wings have a slightly negative α, suspected to reduce induced drag. Overall twist has a linear distribution from 0 deg at the center to $+5$ deg at the fifth digit to -2 deg at the tip.

B. Computational Results

Working with prestalled performance based on airfoil studies, Weissinger analysis sweeps from -2 deg to 12 deg α by increments of 0.2 deg. Lift coefficient versus α for the flat unmorphed and cambered, and twisted morphed wings is shown in Fig. 3, and lift-to-drag ratio versus α for both configurations is compared in Fig. 4. The morphed shape is strongly favored in these plots. Both lift and lift to drag are higher in the morphed configurations for each species across all α. Maximum lift coefficient increases over 50% for each species when morphed. Because of increased camber through morphing, drag coefficient (not pictured) also increases; however, lift-to-drag ratio still increases around 34% in the morphed shape for each species. Further details of this study are given in Leylek et al. [25].

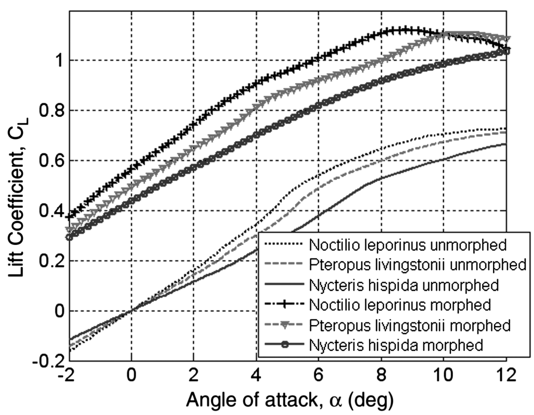

Fig. 3 Lift coefficient vs α for morphed and unmorphed wings.

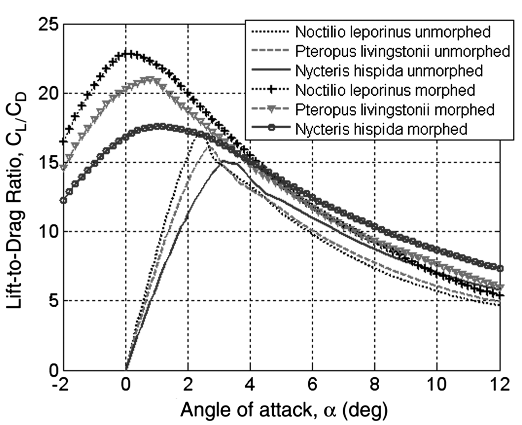

Fig. 4 Lift-to-drag ratio vs α for morphed and unmorphed wings.

Results predicted through Weissinger analysis for morphed configurations correspond well to expected natural flight for the three bat species. *Noctilio leporinus* has the highest lift coefficient, fitting, given its need to carry prey. It also has high lift-to-drag ratio, which would be consistent with its nature, as it must have efficient flight to commute to water sources. *Pteropus livingstonii* also has high lift-to-drag ratio, expected, because efficiency is necessary for soaring, but aspect ratio is lower than that of *N. leporinus*. Insectivorous *Nycteris hispida* must be agile and maneuverable, and it has evolved its wing shape as such. Its wings have forward sweep, causing the inboard wing portion to stall first. This sweep allows it to maintain roll control and resist spins by using outboard fingers to control camber [26]. As noted by Raymer [27], combination of these effects delays overall wing stall, as does its low aspect ratio. It has the lowest peak lift-to-drag ratio of the three species, though at high α lift to drag is highest. This high α advantage allows for higher bank angles and more extreme turn capabilities than other bats. Lift distributions in Fig. 5 also give insight to *N. hispida*'s maneuverability; peaks center in the middle of each wing for the more efficient *N. leporinus* and *P. livingstonii*, whereas with *N. hispida* lift concentrates toward the tips.

IV. Experimental Validation

A. Experimental Methods

To assess Weissinger method accuracy, wind tunnel models of morphed and unmorphed *Pteropus livingstonii* wings were fabricated using a Stratasys Dimension rapid prototyper of acrylonitrile butadiene styrene plastic, with steel dowels for added rigidity. Wings connect to an aerodynamic sting atop a 6 deg-of-freedom JR3 load cell, which measures lift to 25 lb with a resolution of less than 0.01 lb. Tests use the Cornell University environmental wind tunnel facility, an open return wind tunnel with a $48'' \times 43''$ test section. Test speeds

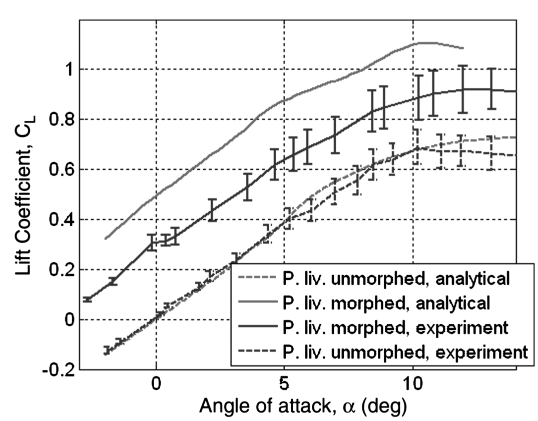

Fig. 6 Lift coefficient vs α for morphed and unmorphed configurations of *P. livingstonii*.

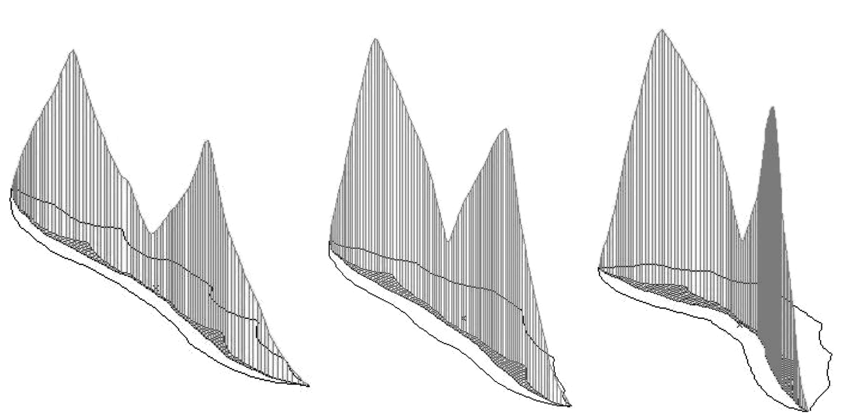

Fig. 5 Lift distributions across the wings of *N. leporinus*, *P. livingstonii*, and *N. hispida* (left to right).

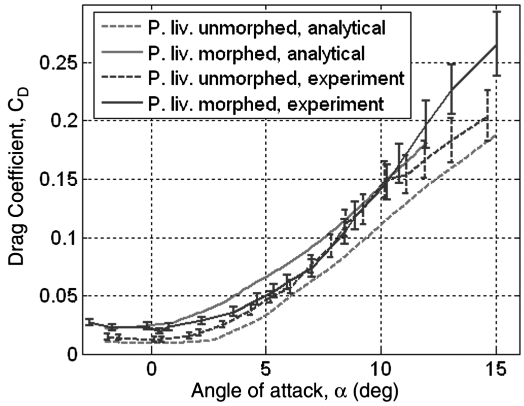

Fig. 7 Drag coefficient vs α for morphed and unmorphed configurations of *P. livingstonii*.

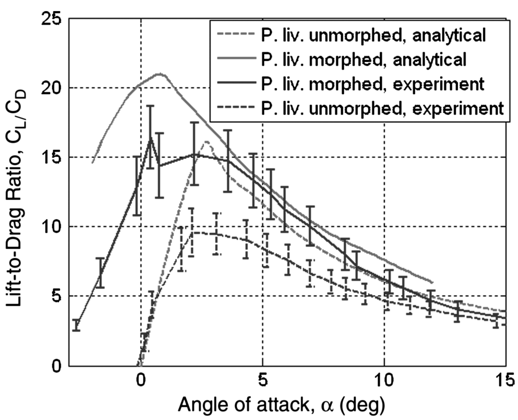

Fig. 8 Lift-to-drag ratio vs α for morphed and unmorphed configurations of *P. livingstonii*.

are approximately 10.8 m/s (24 mph), with α ranging from -2 deg to 14 deg by increments of about 1 deg. Lift, drag, and pitch data are sampled at 250 Hz for 90 s at each α, and a Butterworth filter with cutoff frequency at 20 Hz filters tunnel noise.

B. Results

Figures 6–8 show experimental data compared with computational results. The $1-\sigma$ bounds from filtered data are also shown. Because the Weissinger method has limitations discussed in Sec. III, it was expected that analysis would not capture exact values but rather trends, as is apparent in results. In Fig. 7, computed drag is within experimental error for the unmorphed wing, proving the Weissinger method numerically accurate for this simple case. Experiments confirm that lift and drag coefficients are higher for the morphed wing than unmorphed. Lift coefficient increases more than drag coefficient, such that lift-to-drag ratio is higher with morphed shape. The maximum lift-to-drag ratio occurs at the same α in computational and experimental results, indicating a correlation with the Weissinger method.

Experimental results show a 34% increase in maximum lift coefficient and a 72% increase in maximum lift-to-drag ratio, compared with 51% and 30%, respectively, through Weissinger analysis. Although experimental maxima are less than anticipated results from analysis, significant improvements exist in the morphed topology compared with unmorphed.

C. Accuracy of Results

Errors in experimental results come in part from the wind tunnel, which can have an unsteady and changing flow. There is also some degree of turbulence in the wind tunnel, and the wing surface may not be perfectly smooth. The thin, plastic model is subject to vibrations, some of which are removed through filtering. The method of measuring α is imperfect, causing the entire lift curve to be shifted up to 1 deg along the α-axis. Though area blockage and side wall effects are minimal, the wing height-to-span ratio is only 0.5, placing it in ground effect and increasing lift coefficients above their true values.

V. Optimization

A. Optimization Method

Heuristic optimization can determine wing morphing parameters yielding enhanced flight performance and expanded flight envelopes. Here we consider wings optimized without fuselage contributions. Performance metrics are reduced to aerodynamic parameters, similar to optimization of 2-D airfoils [4,16,27]. These metrics and their correlations to flight performance are summarized in Table 1. The bat wing model is modified from the initial guess for morphed configuration of Sec. III.A. The root is again modeled as a nonlifting element, so that a symmetric NACA 0003 with zero twist is maintained in the midsection of the wing. Table 2 provides summary of design parameters and bounds. Camber and twist angles are linearly interpolated between the root and fifth digit, as well as between the fifth digit and wingtip.

To reduce the number of calculations, simulated annealing is chosen as the optimization method, proven robust and reliable in finding global optima [28]. The MATLAB code written and used by Goffe et al. [29] is adapted to the outlined design variables and forms a shell around the extended Weissinger method. As the Weissinger method only allows integer values for camber, all state variables lie in discrete space. This reduces final state accuracy, but also decreases search space size and runtime.

B. Optimization Results

Each cost function was tested three times with different initial morphed wing shapes, ensuring that optimization yields consistent convergence to the global maximum. Results of tested cost functions and improvement over initial guess morphology from Sec. III.B for *P. livingstonii* are presented in Table 3, with other species omitted for brevity. Optimized state follows the order of Table 2.

To maximize lift, the wing morphology approaches the upper bound of all design parameters. Aerodynamic theory predicts that lift is increased as camber, twist, and/or α increases, continuing until flow separates on the upper side of the wing. In agreement with this, optimization yields camber and α at maximum lift before stall.

Table 1 Summary of optimized cost functions and correlations to flight performance

Performance metric	Correlated performance characteristics
1. Maximum lift coefficient	Take off Instantaneous turns Turn radius
2. Minimum drag	Climb Acceleration Dash
3. Maximum lift-to-drag	Cruise range Powered loiter/endurance Sustained turns
4. Minimum power consumption ($C_L^{(3/2)}/C_D$)	Power consumption Gliding endurance Sinking rate

Table 2 Design parameters and their bounds

Parameter and bounds	
1. Camber at wing root	$[0,9] \in \mathbf{Z}$
2. Camber at fifth digit	$[0,9] \in \mathbf{Z}$
3. Twist at fifth digit	$[0,6] \in \mathbf{Z}$
4. Twist at wingtip	$[-3,3] \in \mathbf{Z}$
5. Angle-of-attack, α	$[-2,14] \in \mathbf{Z}$

Table 3 Optimization results for Pteropus livingstonii

Cost	Optimum found	Improvement	State
Maximum lift	1.43	29.40%	[8;9;5;3;14]
Min C_D	0.00920	58.1%	[0;0;0;1;0]
Max C_L/C_D	22.79	8.89%	[6;5;2;−2;2]
Max $C_L^{(3/2)}/C_D$	17.761	13.3%	[6;7;1;0;3]

Optimized wings for each species have not only higher peak lift than the initial guess morphed configuration but higher lift coefficients at every α considered. For both lift-to-drag ratio and $C_L^{3/2}/C_D$ metrics, wings have moderate camber values, coinciding with XFOIL results from Leylek et al. [25], wherein airfoils with 5–7% camber are the most efficient.

Wings optimized for minimum drag are different than those for other flight parameters and more closely resemble the unmorphed shape. With minimum drag, all three species need very slight or no camber, a tip twist of 1 or 2 deg, and a small cruise α of 0 to 2 deg, all expected because these almost symmetric wings have minimal lift at this α and minimal lift-induced drag. The drag metric reveals the necessity for wings morphing between symmetric, untwisted shapes when minimum drag is critical and with added camber and twist for enhancing other metrics. Further results are given in Manzo et al. [30].

In general, performance improves by the same amount for wing planforms representing each species. For example, in all three planforms, drag decreases by about 60% after morphed shape optimization. Trends between species generally remain the same: *N. leporinus* has highest lift-to-drag ratio and *N. hispida* has the lowest, except at higher α, as with the behavior of initial guess morphologies. This suggests that wing shape characteristics such as aspect ratio and tip shape have a dominant effect in determining and limiting flight performance of a particular bat species.

VI. Conclusions

This research adapts bats' characteristic planforms and morphological change capabilities to man-made fixed wings with future morphing potential. Even using an initial guess for bat wing shape change, morphing from a flat to cambered and twisted state yields significant lift and efficiency improvements. Experimental snapshot data of morphed and unmorphed wing states validate qualitative trends seen through analysis, whereas morphed shape optimization further expands capabilities by prescribing shape change suited not just to ecological niche, but to maximizing key flight parameters. Whereas the piscivorous *Noctilio leporinus* has the best lift-to-drag ratio and endurance characteristics, its maximum lift and minimum drag are very close to those achieved by the soaring *Pteropus livingstonii*. Agile *Nycteris hispida* has the best performance relative to the other two bat species at high angles of attack, useful for navigation in tight spaces. Results define morphologies that batlike wings should adopt for different mission objectives and can inform actuator requirements in terms of deflection, sizing, and load carrying capability. Findings indicate that engineered wings inspired by bat planforms and morphologies can provide significant merits to the aerospace community, in terms of both aerodynamic efficiency and an increased and highly adaptable flight envelope.

References

[1] Norberg, U. M., Brooke, A. P., and Trewhella, W. J., "Soaring and Non-Soaring Bats of the Family Pteropodidae (Flying Foxes, Pteropus Spp.): Wing Morphology and Flight Performance," *Journal of Experimental Biology*, Vol. 203, No. 3, 2000, pp. 651–664.

[2] Norberg, U. M., and Rayner, J. M. V., "Ecological Morphology and Flight in Bats (Mammalia; Chiroptera): Wing Adaptations, Flight Performance, Foraging Strategy and Echolocation," *Philosophical Transactions of the Royal Society of London. Series B, Biological Sciences*, Vol. 316, No. 1179, 1987, pp. 335–427. doi:10.1098/rstb.1987.0030.

[3] Bullen, R., and McKenzie, N. L., "Bat Airframe Design: Flight Performance, Stability and Control in Relation to Foraging Ecology," *Australian Journal of zoology*, Vol. 49, 2001, No. 3, pp. 235–261. doi:10.1071/ZO00037

[4] Shyy, W., Klevebring, F., Nilsson, M., Sloan, J., Carroll, B., and Fuentes, C., "Rigid and Flexible Low Reynolds Number Airfoils," *Journal of Aircraft*, Vol. 36, No. 3, 1999, pp. 523–529. doi:10.2514/2.2487

[5] Lee, C. S., Pang, W. W., Srigrarom, S., Wang, D., and Hsiao, F., "Classification of Airfoils by Abnormal Behavior of Lift Curves at Low Reynolds Number," *24th Applied Aerodynamics Conference*, AIAA Paper 2006-3179, 2006.

[6] Reid, M. R., and Kozak, J., "Thin/Cambered/Reflexed Airfoil Development for Micro Air Vehicle Applications at Reynolds Numbers of 60,000 to 100,000," AIAA Paper 2006-6832, 2006.

[7] Willis, D. J., Persson, P., Israeli, E. R., Peraire, J., Swartz, S. M., and Breuer, K. S., "Multifidelity Approaches for the Computational Analysis and Design of Effective Flapping Wing Vehicles," AIAA 2008-518, 7–10 Jan. 2008.

[8] Swartz, S. M., Iriarte-Diaz, J., Riskin, D. K., Song, A., Tian, X., Willis, D. J., and Breuer, K. S., "Wing Structure and the Aerodynamic Basis of Flight in Bats," AIAA 2007-42, 8–11 Jan. 2007.

[9] Bunget, G., "BATMAV: A Biologically-Inspired Micro-Air Vehicle for Flapping Flight," Masters Thesis, North Carolina State Univ., Raleigh, NC, 2007.

[10] Song, A. J., and Breuer, K. S., "Dynamics of a Compliant Membrane as Related to Mammalian Flight," AIAA Paper 2007-665, 8–11 Jan. 2007.

[11] Ifju, P. G., Jenkins, D. A., Ettinger, S., Lian, Y., Shyy, W., and Waszak, M. R., "Flexible-Wing-Based Micro Air Vehicles," AIAA Paper 2002-0705, 14–17 Jan. 2002.

[12] Lian, Y., and Shyy, W., "Numerical Simulations of Membrane Wing Aerodynamics for Micro Air Vehicle Applications," *Journal of Aircraft*, Vol. 42, No. 4, 2005, pp. 865–873. doi:10.2514/1.5909

[13] Garcia, H. M., Abdulrahim, M., and Lind, R., "Roll Control for a Micro Air Vehicle Using Active Wing Morphing," AIAA Paper 2003-5347, 11–14 Aug. 2003.

[14] Wlezien, R. W., Horner, G. C., McGowan, A. R., Padula, S. L., Scott, M. A., Silcox, R. J., and Simpson, J. O., "The Aircraft Morphing Program," AIAA Paper 98-1927, 1998.

[15] Bowman, J., Sanders, B., and Weisshaar, T., "Evaluating the Impact of Morphing Technologies on Aircraft Performance," AIAA Paper 2002-1631, 2002.

[16] Joshi, S. P., Tidwell, Z., Crossley, W. A., and Ramakrishnan, S., "Comparison of Morphing Wing Strategies Based Upon Aircraft Performance Impacts," AIAA Paper 2004-1722, 2004.

[17] Leylek, E. A., Manzo, J. E., and Garcia, E., "A Bat-Wing Aircraft Using the Smart Joint Mechanism," *Advances in Science and Technology*, Vol. 58, 2008, pp. 41–46. doi:10.4028/www.scientific.net/AST.58.41.

[18] Manzo, J. E., and Garcia, E., "Methodology for Design of an Active Rigidity Joint," *Journal of Intelligent Material Systems and Structures*, Vol. 20, 3, 2008, pp. 311–327. doi:10.1177/1045389X08093826

[19] Norberg, U. M., "Some Advanced Flight Manoeuvres of Bats," *Journal of Experimental Biology*, Vol. 64, 2, 1976, pp. 489–495.

[20] Pennycuick, C. J., "Gliding Flight of the Dog-Faced Bat Rousettus Aegyptiacus Observed in a Wind Tunnel," *Journal of Experimental Biology*, Vol. 55, 1971, pp. 833–845.

[21] Norberg, U. M., "Morphological Adaptations for Flight in Bats," *Bat Biology and Conservation*, Smithsonian Inst. Press, Washington, DC, 1998, pp. 93–108.

[22] Neuweiler, G., *The Biology of Bats*, Oxford Univ. Press, New York, 2000, pp. 9–40.

[23] Wickenheiser, A. M., and Garcia, E. "Aerodynamic Modeling of Morphing Wings Using an Extended Lifting-Line Analysis," *Journal of Aircraft*, Vol. 44, No. 1, 2007, pp. 10–16. doi:10.2514/1.18323

[24] Drela, M., "XFOIL: An Analysis and Design System for Low Reynolds Number Airfoils," *Low Reynolds Number Aerodynamics*, Springer–Verlag, New York, 1989, pp. 1–12.

[25] Leylek, E. A., Manzo, J. E., and Garcia, E., "Analysis of Bat Wings for Morphing," *Proceedings: Active and Passive Smart Structures and Integrated Systems II*, Vol. 6928, SPIE, San Diego, CA, 10–13 March 2008.

[26] Pamadi, B. N., *Performance, Stability, Dynamics, and Control of Airplanes*, AIAA, Reston, 1998, p. 56.

[27] Raymer, D. P. *Aircraft Design: A Conceptual Approach*, AIAA, Washington, DC, 1989, pp. 549.

[28] Corona, A., Marchesi, M., Martini, C., and Ridella, S., "Minimizing Multimodal Functions of Continuous Variables with the 'Simulated Annealing' Algorithm," *ACM Transactions on Mathematical Software*, Vol. 13, No. 3, 1987, pp. 262–280. doi:10.1145/29380.29864

[29] Goffe, W. L., Ferrier, G. D., and Rogers, J., "Global Optimization of Statistical Functions with Simulated Annealing," *Journal of econometrics*, Vol. 60, No. 1–2, 1994, pp. 65–99.

[30] Manzo, J. E., Leylek, E. A., and Garcia, E., "Drawing Insight from Nature: A Bat Wing for Morphing Aircraft," *ASME Conference on Smart Materials, Adaptive Structures and Intelligent Systems*, 2, SMASIS2008-613, ASME, Ellicott City, MD, 28–30 Oct. 2008, pp. 671–678.

I. Chopra
Associate Editor